[15]J. R. Burke, B. B. Houston, H. T. Savage, J. Babiskin, and P. G. Siebenmann, Phys. Soc. Japan Suppl. 21, 384 (1966).
[16]R. S. Allgaier (unpublished).

PHYSICAL REVIEW B VOLUME 2, NUMBER 4 15 AUGUST 1970

High-Field Conductivity of the ⟨111⟩ Valleys of Ge

W. P. Dumke
IBM *Watson Research Center, Yorktown Heights, New York* 10598
(Received 6 February 1970)

We have calculated the distribution function and drift velocity of electrons in the ⟨111⟩ valleys of Ge. The model used is essentially a one-valley model for an electric field in the [100] direction and without any electron transfer to higher valleys. The nonparabolicity of the conduction band and the nonclassical occupation of the acoustic modes are taken into account. The coupling constants were obtained from a fit to the low-field mobility, and because of the inclusion of nonparabolicity, the optical-mode coupling was smaller than previously used. The calculated drift velocity is in excellent agreement with the results of Ruch and Kino, and shows a low-temperature negative resistance which vanishes at somewhat above 77 °K. Although the electron energies at an electric field of several thousand V/cm indicate that some electron transfer to higher valleys is probably taking place, it is likely that this transfer is not primarily responsible for the observed negative resistance, but rather results in the resumption of a positive conductivity at still higher electric fields.

I. INTRODUCTION

The discovery of current oscillations in n-type Ge by McGroddy and Nathan[1] and the subsequent observation of a negative resistance in the bulk I-V characteristics[2,3] have resulted in a renewed interest in the electrical conductivity of Ge.

In comparison with the negative conductance observed in the I-V characteristics of GaAs, the negative conductance in Ge with the electric field along a ⟨100⟩ direction is relatively small and decreases with increasing temperature, vanishing at somewhat above 100 °K.

Theoretically, the conductivity properties of n-type Ge and GaAs should differ significantly in detail, since they depend upon features of the band structure and upon scattering mechanisms which are considerably different in the two materials. In GaAs, with its dominant polar optical-mode electron scattering mechanism, the drift velocity of electrons in the central minimum shows little tendency to reach a limiting value for electric fields at which electron transfer is unimportant. At higher fields (>3000 V/cm) electrons increasingly transfer to states in the ⟨100⟩ minima which have a considerably greater density of states than in the lowest conduction minimum and a much lower mobility. The electron transfer mechanism, therefore, acts rather effectively to produce a negative resistance in GaAs.

In Ge, electron transfer is also possible, but the effect on the electrical conductivity should be less drastic than in GaAs, because the densities of states and drift velocities of the upper and lower minima are not greatly different in Ge. In Ge, however, which is nonpolar, the drift velocity would be expected, under certain assumptions,[4] to reach a limiting value without electron transfer, so that even a small modification of the I-V characteristics due to transfer could cause a negative resistance.

The assumptions which yield a limiting drift velocity in Ge are not exactly obeyed, and it is important to accurately know the drift velocity of the electrons in the lowest minima if we are to understand the over-all I-V characteristics. In spite of some transfer to the ⟨100⟩ valleys, the electrons in the ⟨111⟩ valleys probably constitute a majority of the carriers over most of the negative-resistance region of interest.

The pressure experiment of Melz and McGroddy[5] is, in fact, qualitatively consistent with the model whereby the negative resistance in Ge is removed rather than produced by electron transfer to higher valleys. They found that the reduction by hydrostatic pressure of the separation between the ⟨111⟩ and ⟨100⟩ valleys was accompanied by a decrease in the amplitude of oscillations and an increase in

the electric field threshold. The decrease in the valley separation would be expected to facilitate electron transfer and thereby lower the threshold field, if transfer was responsible for the oscillation-producing negative resistance.

To more accurately assess the contribution to a negative resistance of the electrons in the ⟨111⟩ valleys in Ge, we have calculated their distribution function and drift velocity with an electric field in the [100] direction *without* employing the following simplifying approximations:

Parabolicity of E versus $\vec{k}$ *in conduction band.* We have assumed a hyperbolic E versus $\vec{k}$ relationship characteristic of a direct energy gap of 1.54. This is a slightly greater nonparabolicity than is given by the observed direct gap of 2.2 eV.[6] However, the 1.54-eV value corresponds to the mass variation observed by Aggarwal *et al.*[7] in magnetopiezotransmission experiments. The nonparabolicity enters into the calculation of the group velocity, density of states, etc. To be consistent, we have also included the decrease in the overlap of the cell periodic part of the wave functions between initial and final states in calculating the scattering probability for electrons. The effect of nonparabolicity on the I-V characteristic is to produce a negative resistance, since the effective mass increases with electron energy.

Elastic acoustic-mode scattering. In this approximation, the energy loss due to the acoustic-mode phonons is ignored, and the acoustic modes are assumed to be classically excited. This is not a very good approximation when the energy of the electrons becomes large and the separation in $\vec{k}$ space between initial and final states, and therefore the phonon energies, becomes appreciable. We shall take into account the energy lost due to acoustic-mode scattering. This is a mechanism for which the rate of energy loss increases more rapidly than with optical-mode scattering, and therefore it disposes the electrical characteristics towards a positive resistance. We will also calculate more exactly the scattering by the acoustic modes. This is necessary since a moderately energetic electron will be able to interact with acoustic-mode phonons of considerable energy. For a 0.1-eV electron in Ge with a longitudinal effective mass $m_L = 1.58m$, where m is the free-electron mass, and a velocity of sound $s = 5\times10^5$ eV/sec, the phonon energies range up to

$$k\theta = s\times 2\,(2m_L E)^{1/2} = 0.013 \text{ eV} \quad \text{or} \quad \theta = 150\ ^\circ\text{K}\ .$$

At the lower temperatures such modes are not classically excited, and at the lowest temperatures spontaneous acoustic-mode emission dominates acoustic-mode scattering. Because the scattering rate for spontaneous acoustic-mode emission increases at a more rapid rate with increasing electron energy than does acoustic-mode scattering with classically excited modes, the scattering by spontaneous emission contributes to a negative resistance.

Although we have removed several approximations which might obscure the existence of a negative-resistance characteristic, we have retained or have adopted several other approximations which will be discussed as they occur in the mathematical treatment.

II. MATHEMATICAL TREATMENT: BAND STRUCTURE

The conduction-band structure of Ge is well known.[8] There are four equivalent valleys located along the ⟨111⟩ directions in $\vec{k}$ space, with the minima at the Brillouin-zone faces. The longitudinal mass m_L along the [111] direction is much larger than the transverse mass m_T. The curvature in the transverse direction is mainly due to a $\vec{k}\cdot\vec{P}$ repulsive interaction with a valence band of symmetry L_3^- approximately 2.2 eV below the conduction minima.[9] When two bands have a strong exclusive mutual interaction determining their curvatures, Kane[10] has shown that the resulting E-versus-$\vec{k}$ dependence will by hyperbolic in form (apart from the free-electron term) rather than parabolic. These conditions will approximately be met for the dependence of E on transverse $\vec{k}$ (k_x,k_y) in Ge. Neglecting the free-electron term, this dependence is given by

$$E = \tfrac{1}{2}E_G\left(\left\{1+\left[2\hbar^2(k_x^2+k_y^2)/E_G m_T\right]\right\}^{1/2}-1\right). \quad (1)$$

Aggarwal, Zuteck, and Lax[7] found that the cyclotron resonance transverse effective mass varied in a manner consistent with Eq. (1), but corresponded to a somewhat greater degree of nonparabolicity, which is given by a value of $E_G = 1.54$ eV. This enhanced nonparabolicity is understandable if there is a partial cancellation of the curvature produced due to the L_3^- valence band by a higher-lying conduction band.

We shall assume that the form of the E-versus-$\vec{k}$ dependence in the longitudinal direction is the same as that for the transverse direction. The dependence of E on $\vec{k}$ is therefore given by

$$E = \tfrac{1}{2}E_G\left(\left\{1+(2\hbar^2/E_G)\left[\vec{k}\cdot(\overleftrightarrow{m}^*)^{-1}\cdot\vec{k}\right]\right\}^{1/2}-1\right), \quad (2a)$$

where $(\overleftrightarrow{m}^*)^{-1}$ is a tensor inverse mass given by

$$(\overleftrightarrow{m}^*)^{-1} = \begin{pmatrix} m_T & 0 & 0 \\ 0 & m_T & 0 \\ 0 & 0 & m_L \end{pmatrix}$$

in the principle-axis system of a valley. Although we shall evaluate certain quantities considering

the geometry of the actual energy surfaces, it will for the most part be convenient to transform the ellipsoidal energy surfaces to spheres, using the transformation[11] $\vec{k}=(m_c/\overleftrightarrow{m}^*)^{1/2}\cdot\vec{k}$, where the conductivity mass m_c is given by

$$m_c=[\tfrac{1}{3}(2/m_T+1/m_L)]^{-1}\ .$$

Equation (2a) becomes

$$E=\tfrac{1}{2}E_G[(1+2\hbar^2\vec{k}^2/E_G m_c)^{1/2}-1]\ . \tag{2b}$$

In the transformed coordinates we may also write the following expressions:

$$V^2=\left(\frac{\partial E}{\partial\hbar\vec{k}}\right)^2=\left(\frac{\hbar\vec{k}}{m_c}\right)^2\Big/\left(1+\frac{2\hbar^2\vec{k}^2}{m_cE_G}\right)^2$$

$$=\frac{2E}{m_c}\frac{(1+E/E_G)}{(1+2E/E_G)^2}\ , \tag{3}$$

$$(\hbar\vec{k})^2=2m_cE(1+E/E_G)\ , \tag{4}$$

and per valley and spin, the density of states is given by

$$\rho(E)=4\pi\vec{k}^2m_Tm_L^{1/2}/(2\pi)^3\left|\frac{\partial E}{\partial\vec{k}}\right|m_c^{3/2}$$

$$=(m_Tm_L^{1/2}/2^{1/2}\pi^2\hbar^3)E^{1/2}R(E)\ , \tag{5}$$

where $R(E)=(1+E/E_G)^{1/2}(1+2E/E_G)$.

$R(E)$ is the ratio of the hyperbolic and parabolic densities of states.

III. SCATTERING MECHANISMS

The scattering probability for nonpolar acoustic-mode scattering is of the form

$$P_{\vec{k},\vec{k}+\vec{q}}=A\cdot\hbar\omega\ \mathcal{O}^2[N\delta(E'+\hbar\omega-E)$$

$$+(N+1)\delta(E'-\hbar\omega-E)], \tag{6}$$

where $\mathcal{O}=\int u^*_{\vec{k}+\vec{q}}u_{\vec{k}}dV$

and $N=1/[\exp(\hbar\omega/kT)-1]$.

Here $\hbar\omega$ is the energy of acoustic waves of wave number $\pm\vec{q}$ capable of scattering an electron from an initial state of wave number $\vec{k}$ to a state of wave number $\vec{k}+\vec{q}$ by either the absorption of a phonon (N) or the emission of a phonon ($N+1$).

There are several approximations usually made in the treatments of acoustic-mode scattering probability: (i) to ignore the acoustic-mode phonon energy, since $\hbar\omega\ll E$, and consider the initial and final states to be equal in energy; (ii) to expand the Bose function for N, assuming that $\hbar\omega\ll kT$ and therefore that $N\gg1$; (iii) to assume that $\mathcal{O}=1$ and ignore the decrease in overlap between initial and final states as $\vec{q}$ becomes larger. We shall make only approximation (i), although we will not neglect the energy lost to the acoustic modes.

The variation of the scattering probability, because of the decrease of overlap with increasing phonon wave number, eliminates much of the enhancement of the scattering rate which occurs because of the greater increase with energy of the density of states in a hyperbolic band as compared to a parabolic band. Matz[12] has considered the decrease of this overlap in a two-band system, and we have used his expression for the variation of the overlap and have evaluated its effect upon the rates of energy loss and momentum loss. The use of Matz's result involves the assumption that the amount of L-point wave functions mixed into that for the conduction band is the same in the longitudinal direction as the transverse at a given energy. The deficiencies of our knowledge of the mixing and curvature of the conduction-band states in the longitudinal direction can be shown to result in relatively little uncertainty in the drift velocity. This is because (i) the effects due to the decrease in overlap on the energy loss rate and the momentum loss rate approximately cancel in the drift velocity and (ii) the conductivity effective mass is largely determined by the transverse effective mass. The expression given by Matz for the square of the overlap $\mathcal{O}$, using the expansion coefficients given by Kane[10] for two bands, becomes

$$\mathcal{O}^2=(1/4\eta^2)[(\eta+E_G)^2+2(\eta^2-E_G^2)\cos\theta$$

$$+(\eta-E_G)^2\cos^2\theta+\tfrac{1}{12}(\eta-E_G)^2(1-\cos^2\theta)]\ , \tag{7}$$

where $\eta=E_G+2E$, $|\vec{K}|=|\vec{K}'|$, and $\cos\theta$ is the angle between $\vec{K}$ and $\vec{K}'$ (in the transformed coordinates).

The decrease in overlap will affect the momentum and energy loss rates in slightly different ways. Since the overlap correction increases with the angle of scattering, the effect of this correction on the momentum loss will be greater than for a mechanism which is not dependent on the angle, i.e., nonpolar optical-mode energy loss. The overlap correction for the momentum relaxation rate is given by

$$M(E)=(\pi)^{-1}\int_0^\pi(1-\cos\theta)\left|\mathcal{O}^2\sin\theta\,d\theta\right.\ , \tag{8}$$

where we assume that the scattering will be isotropic. In Fig. 1 we compare the decrease in the overlap function of the increasing electron energy with the inverse of the change in the density of states obtained in going from a parabolic band to a hyperbolic band. The very close agreement between these two curves leads to a computational simplification in which the corrections in the mo-

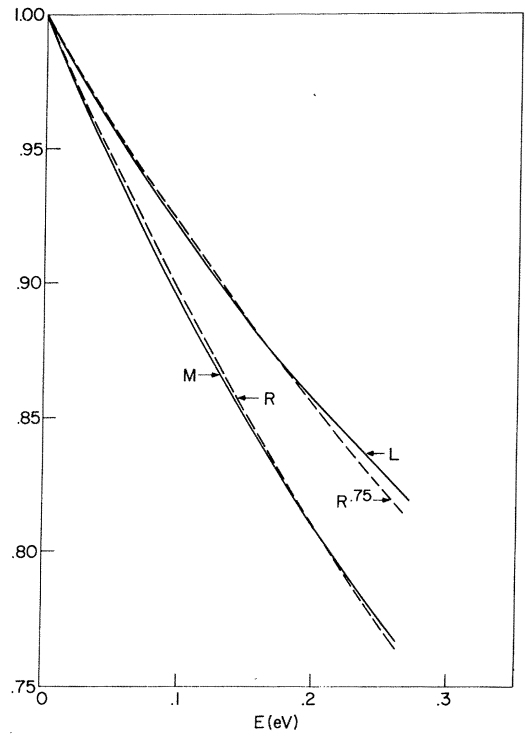

FIG. 1. Effects of nonparabolicity versus electron energy in the conduction band of Ge. R is the increase in the electron effective mass due to nonparabolicity, L is the overlap factor $\mathcal{O}^2$ averaged over an energy surface, and M involves an average of this factor weighted by $(1-\cos\theta)$.

mentum relaxation time for overlap and the correction for a hyperbolic-band density of states are taken as exactly cancelling, that is $M(E)R(E)=1$.

The average overlap correction for optical-mode energy loss is somewhat smaller since it involves an unweighed average over an energy surface. This correction $L(E)=\bar{\mathcal{O}}^2$ is also plotted in Fig. 1 along with $R(E)^{-3/4}$ for the sake of comparison.

In treating the acoustic-mode scattering more exactly, we have, nevertheless, made several convenient approximations. The momentum relaxation rate consists of the scattering with spontaneous phonon emission and the induced scattering processes and is of the form

$$\frac{1}{\tau}=\frac{1}{2}A\int\left(1-\frac{k_\epsilon'}{k_\epsilon}\right)\hbar s\,|\vec{k}-\vec{k}'|\,\delta(E_{\vec{k}}-E_{\vec{k}'})\frac{d^3k'}{(2\pi)^3}$$
$$+A\int\left(1-\frac{k_\epsilon'}{k_\epsilon}\right)\frac{\hbar s\,|k-k'|}{\exp(\hbar s\,|\vec{k}-\vec{k}'|/kT)-1}$$
$$\times\delta(E_k-E_{k'})\frac{d^3k'}{(2\pi)^3}\ , \qquad (9)$$

where k_ϵ is the component of $\vec{k}$ along the electric field. If we had spherical energy surfaces, the first term could be integrated analytically and would give $\frac{3}{5}A\rho(E)\hbar s\bar{k}$, where $\bar{k}$, the average value of the phonon wave number for a spherical surface of radius k_r easily shown to be $\frac{4}{3}k_r$.

The second term involves an integral over Bose functions for various phonon wave numbers and energies. For the smallest angle scattering or at very high lattice temperatures the term in the scattering probability of the form

$$\frac{\hbar s\,|\vec{k}-\vec{k}'|}{\exp(\hbar s\,|\vec{k}-\vec{k}'|/kT)-1}$$

is expandable and becomes simply proportional to kT. Under most hot-electron conditions this approximation cannot be made and the second term cannot be analytically evaluated.

We have adopted an approximate method for evaluating this term. In this method we see how closely a distribution of Bose functions can be fitted by single function for a phonon wave number characteristic of the dimensions of the energy surface in $\vec{k}$ space. This approximation is similar to the Einstein approximation in the early theory of lattice specific heats. If γ is a constant of order unity, we find that the second term of Eq. (9) can be very closely approximated for spherical surfaces by

$$A\rho(E)\frac{\gamma\hbar sk_r}{\exp(\gamma\hbar sk_r/kT)-1}\ .$$

We show the accuracy of this approximation in Fig. 2 for $\gamma=1.45$. We should emphasize that this type of approximation is not really essential to these calculations, but greatly reduces the amount of computation involved while introducing only a small error.

Due to the ellipsoidal energy surfaces of the Ge valleys the integrals in the acoustic-mode scattering rate are slightly more complicated in their evaluation. They must be evaluated for the field components along each of the principal directions of the valleys, and the distribution of phonon energies depends on the initial state $\vec{k}$ as well as the final state $\vec{k}'$. If we numerically evaluate the first and second terms in Eq. (9) for ellipsoidal surfaces appropriate to Ge, we find, in terms of $k_L=(\hbar)^{-1}(2m_LE)^{1/2}$, that to a very good approximation

$$\frac{1}{\tau}=A\rho(E)\left(\tfrac{1}{2}\hbar s\,0.78k_L+\frac{\hbar s\,0.7k_L}{\exp(\hbar s\,0.7k_L/kT)}-1\right). \qquad (10)$$

We have assumed an electric field in the [100] direction making equal angles with the longitudinal and the two transverse ellipsoid axes, and have weighted the results for longitudinal and transverse fields by the corresponding reciprocal effective-mass elements. For conditions under which $\hbar sk_L \ll kT$ the acoustic-mode scattering rate clearly be-

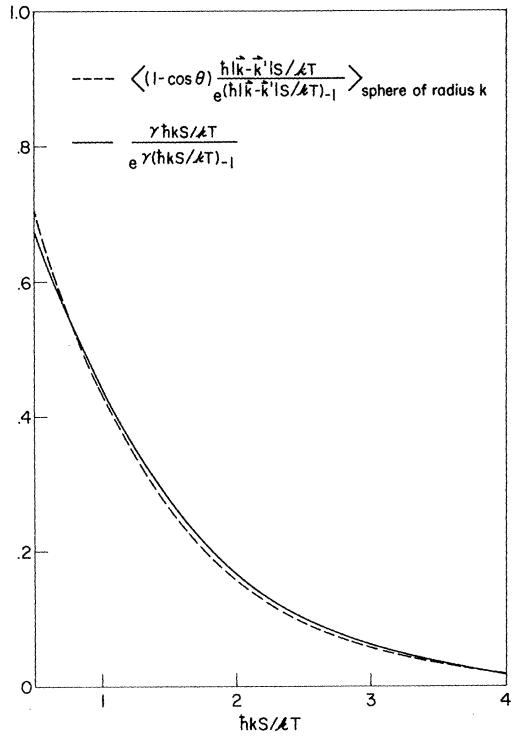

FIG. 2. Approximation for the contribution to momentum scattering by nonclassically excited acoustic modes. The exact integral over modes with various phonon energies and degrees of excitation is represented to a reasonable approximation by scattering by modes with a single-phonon energy proportional to the dimensions of the energy surface in $\vec{k}$ space. The above curves are for spherical energy surfaces, although scattering over ellipsoidal surfaces is treated similarly.

comes $WkT(E/\hbar\omega_0)^{1/2}$.

If we include the overlap correction and the optical-mode scattering, the momentum relaxation time can be written

$$\frac{1}{\tau} = W\Bigg\{\hbar s k_L\left(0.39+\frac{0.7}{\exp(0.7\hbar s k_L/kT)-1}\right) \times (E/\hbar\omega_0)^{1/2} + B\left[N_0(E/\hbar\omega_0+1)^{1/2} + (N_0+1)(E/\hbar\omega_0-1)^{1/2}\right]\Bigg\}, \tag{11}$$

where $N_0=[\exp(\hbar\omega_0/kT)-1]^{-1}$. Here B is the ratio of the optical-mode coupling constant to the acoustic-mode coupling constant W and $\hbar\omega_0$ is the optical-mode energy.

The coupling constants are determined by adjusting W and B to fit the observed low-field mobility between 100 and 300 °K. We write the low-field mobility as

$$\mu = \frac{e}{3kT}\int V^2\tau e^{-E/kT}\rho(E)\,dE \Big/ \int e^{-E/kT}\rho(E)\,dE\ . \tag{12}$$

Because of the effects of nonparabolicity on V^2 and $\rho(E)$, we find that the temperature dependence of μ is somewhat steeper for a given choice of coupling constants than it is when parabolic bands are assumed. The consequence of this is that a smaller component of optical-mode scattering is required to produce a given temperature dependence. We find that a mobility[13] of the form

$$\mu = 3800(T/300)^{-1.67}\ \mathrm{cm}^2/V\,\mathrm{sec}$$

is best fitted by the values $B=0.125$ and $W=4\times10^{12}\ \mathrm{sec}^{-1}$ with $m_c=0.119\ m$. For a parabolic band, the value of $B=0.195$ for the best mobility fit would be significantly larger.

IV. CALCULATION OF DISTRIBUTION FUNCTION

In strong electric fields the electron distribution function ceases to be thermal, but if the fields are not too high the distribution reaches a steady state. The method we shall use to calculate the distribution function is one originally used by Levinson[14] and applied independently to InSb by the author.[15] In this method the net flux of carriers through any energy surface due to the acceleration of the electric field is equated to the downward flux of carriers because of energy loss processes. This amounts to setting up a continuity equation in a one-dimensional energy space, except that the position of a particle can change discontinuously when a phonon is emitted or absorbed.

The total flux through an energy surface due to the electric field $\vec{\mathcal{E}}$ and inelastic scattering may be written $\Phi_{\mathcal{E}}+\Phi_S$. In analogy with the current passing through a surface in real space given by $i=\int\rho\vec{v}\cdot d\vec{s}$, the field-induced flux in $\vec{k}$ space is given by

$$\int \frac{f}{(2\pi)^3}\frac{d\vec{k}}{dt}\cdot d\vec{S}_{\vec{k}}\ .$$

We shall first evaluate $\Phi_{\mathcal{E}}$ for spherical energy surfaces. Using the relation

$$\frac{d\vec{k}}{dt}=\frac{1}{\hbar}e\vec{\mathcal{E}} \quad\text{and}\quad dS_{\vec{k}}=2\pi|k|\vec{k}\sin\theta\,d\theta,$$

where θ is the angle between $\vec{\mathcal{E}}$ and $\vec{k}$, and making the assumption (the diffusion approximation) that

$$f=f_0+f_1\cos\theta\ , \tag{13}$$

where f_0 is isotropic, $\Phi_{\mathcal{E}}$ becomes

$$\Phi_{\mathcal{E}}=\frac{2\pi e\mathcal{E}^2k^2}{(2\pi)^3\hbar}\int_0^\pi(f_0+f_1\cos\theta)\cos\theta\sin\theta\,d\theta\ . \tag{14}$$

The contribution from f_0 vanishes due to symmetry. If we put

$$f_1=-\tau e\mathcal{E}v\frac{\partial f_0}{\partial E}\ ,$$

and use the relation

$$\rho(E) = 4\pi k^2/(2\pi)^3 \hbar v \ ,$$

we obtain

$$\Phi_{\mathcal{E}} = \tfrac{1}{3}\tau(e\vec{\mathcal{E}})^2 v^2 \frac{\partial f}{\partial E}\,\rho(E) \ . \tag{15a}$$

In evaluating $\Phi_{\mathcal{E}}$ for ellipsoidal energy surfaces, θ becomes the angle between $\vec{k}$ and $\vec{\mathcal{E}}$ in the transformed coordinates. The result

$$\Phi_{\mathcal{E}} = \tfrac{1}{3}\tau(e\vec{\mathcal{E}})^2 V^2 \frac{\partial f}{\partial E}\,\rho(E) \tag{15b}$$

is almost identical with (15a) except that V and ρ are those values appropriate to ellipsoidal surfaces given by Eqs. (3) and (5). We shall discuss the accuracy of the diffusion approximation below.

The flux due to scattering is contributed both by the optical modes and the acoustic modes. The first contribution is simply

$$\Phi_{So} = WBI_0(E) = WB\Big[N_0 \int_{E-\hbar\omega_0}^{E} \rho(E')(E'/\hbar\omega_0 + 1)^{1/2} \times R(E' + \hbar\omega_0) L\, dE' - (N_0 + 1)\int_{E}^{E+\hbar\omega_0} \rho(E') \times (E'/\hbar\omega_0 - 1)^{1/2} R(E' - \hbar\omega_0) L\, dE'\Big] \ . \tag{16}$$

The first term includes all those processes in which an electron initially between the energies $E - \hbar\omega_0$ and E absorbs an optical-mode quantum and goes to an energy above E. The second contribution includes processes in which the electron at an energy between E and $E + \hbar\omega_0$ emits an optical-mode phonon and goes to a state below E. The overlap correction factor L between states at E' and $E' + \hbar\omega_0$ was taken to be

$$L = [L(E')L(E' + \hbar\omega_0)]^{1/2} \ .$$

The flux due to the emission of acoustic modes is a smaller but significant part of the total flux. We shall consider only the spontaneous emission processes, since for a hot-electron distribution the flux due to phonon absorption very nearly cancels the flux due to stimulated phonon emission. The spontaneous flux includes all those states which are within an acoustic-mode phonon above the energy surface under consideration. The acoustic flux may be written

$$\Phi_{Sa} = \frac{1}{2} A \iint_{E}^{E+\hbar s|\vec{k}'-\vec{k}|} f(E')\hbar s\,|\vec{k}' - \vec{k}| \times \delta(E' - E - \hbar s\,|k' - k|)\frac{d^3k'}{(2\pi)^6}\,\rho(E')\,dE' \ . \tag{17}$$

If we put $f(E') = f(E)$, since f is slowly varying over a phonon energy, we obtain

$$\Phi_{Sa} = W\rho^2(E)\hbar^2 s^2 \langle |\vec{k} - \vec{k}'|^2 \rangle f(E) \ , \tag{18}$$

where $\langle |\vec{k}' - \vec{k}|^2 \rangle$ is an average of the square of the phonon wave vector averaged over both initial states $\vec{k}$ and final states $\vec{k}'$. For energy surfaces of the shape appropriate to Ge, numerical integration yields for this average $\langle |\vec{k} - \vec{k}'|^2 \rangle = 0.73 k_L^2$.

Having obtained f_0, we may evaluate the drift velocity v_D, where

$$v_D = \frac{e\mathcal{E}}{3m_c} \int E\tau \frac{\partial g}{\partial E}\, e^{-g}\rho(E)\,dE \Big/ \int e^{-g}\rho(E)\,dE \ , \tag{19}$$

and the average energy $\bar{E}$, where

$$\bar{E} = \int E e^{-g}\rho(E)\,dE \Big/ \int e^{-g}\rho(E)\,dE \ . \tag{20}$$

For a steady-state distribution $\Phi_{\mathcal{E}} + \Phi_S = 0$. Inserting Eq. (13) we obtain

$$-\frac{\partial f_0}{\partial E} = \frac{3(\Phi_{So} + \Phi_{Sa})}{(e\mathcal{E})^2 \tau V^2 \rho(E)} \ . \tag{21}$$

If we assume f_0 is of the form $e^{-g(E)}$, we may write

$$-\frac{\partial f_0}{\partial E} = f_0 \frac{\partial g}{\partial E} \ .$$

The distribution function is obtained by iteration. Starting with a trial function, $\partial g/\partial E$ is obtained, yielding a new f_0. To obtain a rapid convergence, the function g_n in the nth trial is of the form

$$g_n(E_i) = \alpha\left[\sum_{j=1}^{i}\left(\frac{\partial g_n}{\partial E}\right)_j \Delta E_j\right] + (1 - \alpha) g_{n-1}(E_i) \ . \tag{22}$$

Computations were facilitated using an IBM model 65 computer in conjunction with a remote APL time-sharing terminal. Because of a limited memory, the number of intervals in energy was limited to approximately 45. At higher energies an analytic extrapolation was used. We estimate that the error in the quantities calculated was approximately 0.2%.

V. RESULTS

In Table I we have summarized some of the values of parameters which were used in these calculations.

TABLE I. Values of the parameters used in this paper.

s	$1.58\,m$
$\hbar\omega_0$	$0.082\,m$
W	1.54 eV
B	4×10^5 cm/sec
m_L	0.0375 eV
m_T	4×10^{12} sec^{-1}
E_G	0.125
$\langle \gamma \lvert k - k' \rvert \rangle$	$0.7k_L$
$\langle \lvert k - k' \rvert^2 \rangle$	$0.73k_L$

The most interesting calculated quantity is the drift velocity, and this is shown in Fig. (3) for a number of temperatures. The calculated results show several qualitative features. At low temperatures there is a negative resistance which starts in the vicinity of 2000 V/cm. The threshold field for the negative resistance increases with increasing temperature, and the magnitude of the negative resistance decreases, apparently vanishing at 150 °K and above. The decrease in the negative resistance is partially due to the increase of the phonon population of the acoustic modes with increasing temperature and partly due to the fact that at higher temperatures the electrons are not as energetic at a given field and therefore are not as strongly affected by nonparabolicity.

We have also plotted the experimental data of Chang and Ruch[3] for 79 °K and that of Gunn[16] for 300 °K. The agreement of the 77 °K curve with the 79 °K data is very good, although the use of the diffusion approximation makes the calculated results suspect, particularly in the region around 1 kV/cm. At higher fields (>4 kV/cm) the distribution becomes more isotropic and the calculated results should be more accurate. The fact that the experimental negative resistance appears to have vanished above 5 kV/cm, whereas the theoretical curves still show a negative resistance, may indicate that the large amount of transfer which can be expected at these fields has largely eliminated the negative resistance.

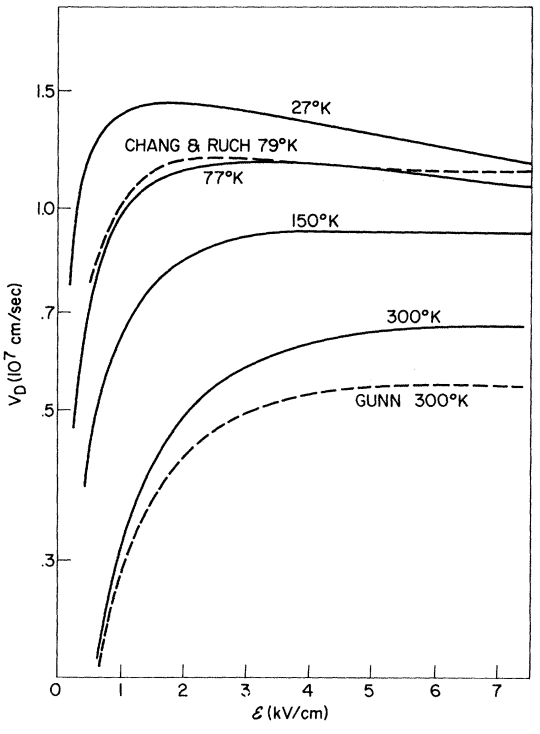

FIG. 3. Drift velocity of electrons versus a [100] electric field in Ge. The solid curves are those calculated for the indicated temperatures. The experimental dotted curves are from Chang and Ruch (Ref. 3) for 79 °K and Gunn (Ref. 16) for 300 °K on Ge of unknown orientation.

The data of Gunn for 300 °K is, unfortunately, from a sample of undetermined crystal direction, and there is also a question of the accuracy of the values. Some more recent data of Smith[17] for the (100) orientation lies about 10% above the Gunn data and are in better agreement with the calculated 300 °K curve. Unfortunately, these data are not very detailed at the lower fields of a few kV/cm. At higher fields the experimental drift velocity nearly saturates, whereas the calculated curve shows a slightly greater increase.

That some transfer is likely over much of the electric field range of interest is apparent from the plot in Fig. 4 of the average electron energy $\bar{E}$ versus electric field at various temperatures. At lower temperatures, the electrons at a given field are more energetic than at higher lattice temperatures. The energy which an electron must have to transfer to the ⟨100⟩ valleys is approximately 0.2 eV,[18] but it is likely that there will be some effects due to transfer when $\bar{E}$ is less than this. At 77 °K $\bar{E}$ is 0.1 eV at 2 kV/cm and 0.2 eV at 3500 kV/cm. At 300 °K, $\bar{E}$ is 0.1 at 3 kV/cm and 0.2 eV at 5.6 kV/cm. It is interesting that, whereas the simple model of hot electrons with momentum and energy loss rates proportional to the density of states in parabolic bands yields a curve of $\bar{E}$ versus $\mathcal{E}$ which goes as $\mathcal{E}^2$ at high fields, the calculated dependence of $\bar{E}$ on $\mathcal{E}$ is nearly linear at high fields.

An indication of the accuracy of our calculations under the assumption that $f = f_0 + f_1 \cos\theta$ can be obtained from Fig. 5 in which the ratio of drift kinetic energy $E_D = \frac{1}{2} m_c v_D^2$ to the average energy $\bar{E}$ is plotted versus field. For either a Maxwellian distribution or a Gaussian, one can show approximately that $E_D/\bar{E} \cong 0.1(f_1/f_0)^2$, and the corresponding approximate value of f_1/f_0 is indicated in Fig. 5.

In conjunction with Price,[19] comparisons have been made between the results of a more simple calculation, using the same method of calculation and truncation approximation used in this paper, with the rigorously exact results obtained using the synchronous ensemble method of Price.[20] There was no significant difference in the values of v_D calculated by the two methods, however the values of f_1/f_0 which occured did not exceed 0.3.

From this comparison we may deduce that our

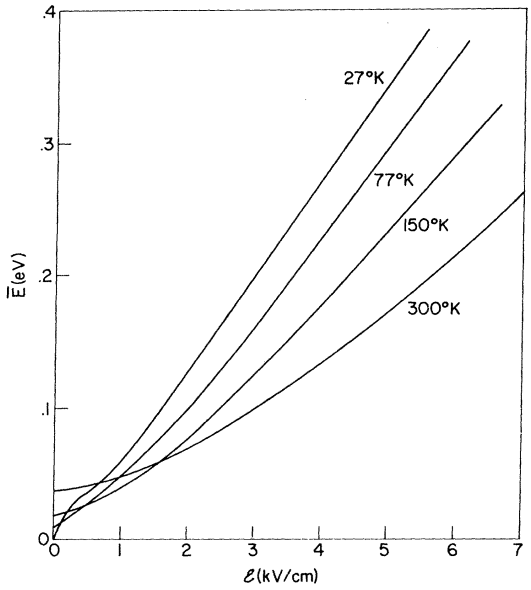

FIG. 4. Average energy $\bar{E}$ versus electric field $\mathcal{E}$ for various temperatures.

calculations for 300 °K are probably not affected significantly by the angular form of the distribution function we have used. This may also be true for the results at high fields and lower temperatures. We do not know what error is introduced by this truncation approximation at lower fields, but the errors should be greatest around 500–1000 V/cm.

Since the drift velocity characteristic we have obtained is a complex result which takes into account several mechanisms usually ignored, it is interesting to consider what the separate influence is on the over-all characteristics of (i) nonparabolicity, (ii) nonclassical acoustic-mode scattering, and (iii) acoustic-mode energy loss.

In Fig. 6 we show drift velocity curves for 77 °K under a variety of assumptions. Curve A is the drift velocity which would be obtained without any of considerations (i), (ii), or (iii). Curve B is obtained with the addition of nonparabolity. For our choice of parameters this appears to be the major effect in providing a negative resistance. In curve C we add the effects of nonclassical excitation of the acoustic modes and, while this also contributes to negative resistance, most of the effect is removed when we take into account the energy lost (really the downward flux in energy) to the acoustic modes in curve D.

The role of the acoustic-mode energy loss in-

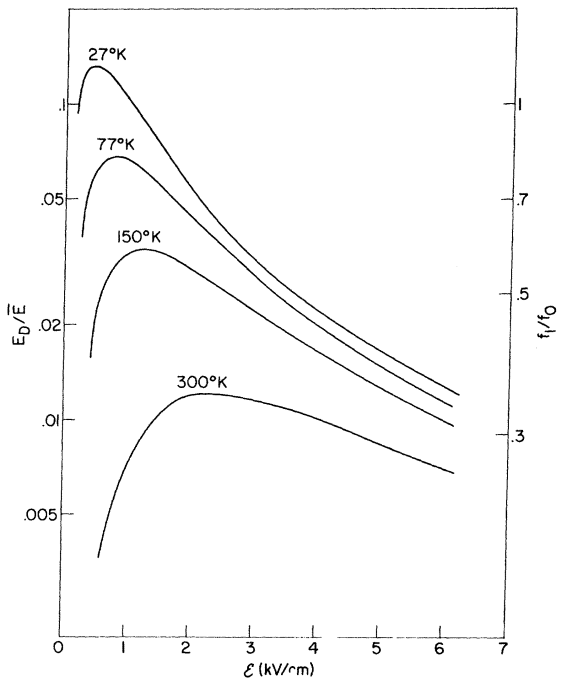

FIG. 5. Kinetic energy of drift $E_D = \frac{1}{2} m_c V_D^2$ relative to $\bar{E}$ and approximate f_1/f_0 versus electric field $\mathcal{E}$.

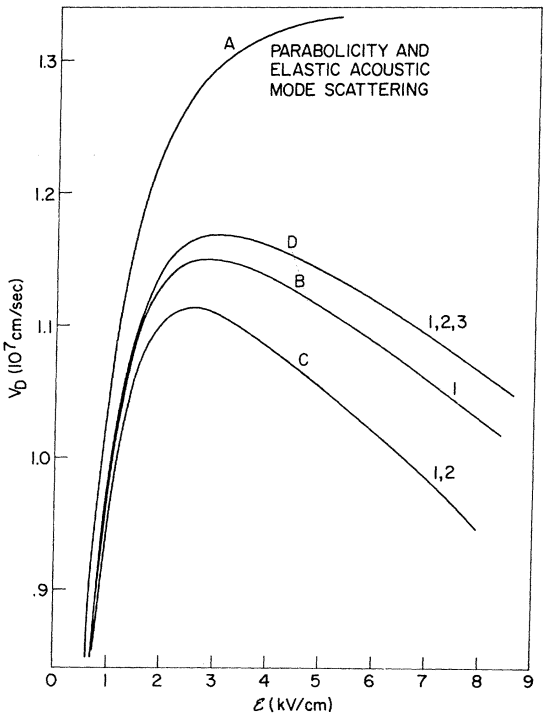

FIG. 6. Drift velocity characteristics obtained under various combinations of the assumptions (i) nonparabolicity, (ii) nonclassically excited acoustic modes, and (iii) acoustic-mode energy loss.

creases with increasing energy. In Fig. 7 we see the fraction of downward flux due to acoustic-mode energy loss versus electron energy. The curves are for a very high field such that $f(E+\hbar\omega_0) \cong f(E)$. The fraction of energy lost to the acoustic modes is typically of the order of 10%. At finite fields the optical-mode loss falls off and the fraction of energy loss due to the acoustic modes is somewhat greater than shown in Fig. 7.

The dependence of the distribution function on energy is somewhat more complicated than the effective-electron-temperature description. At low energies, in the vicinity of $\hbar\omega_0$ and below, the falloff in the distribution is very small because the flux due to the optical modes and the acoustic modes is very small. At high energies the rate of the logarithmic decrease is superlinear because of the effects of nonparabolicity and acoustic-modes energy loss. These features are in evidence in the semilog plot of f_0 versus energy in Fig. 8.

VI. DISCUSSION

The main conclusions we would make from these calculations are the following:

(i) If the most important intraband effects are taken into account, an I-V characteristic results, having the correct magnitude, negative resistance, and temperature dependence of this negative resistance. There is doubt as to accuracy of some of the results where f_1/f_0 is becoming comparable to unity.

(ii) Although the effects of intervalley transfer have been neglected in these calculations, there is probably a significant amount of transfer at the fields considered. It is doubtful, however, that

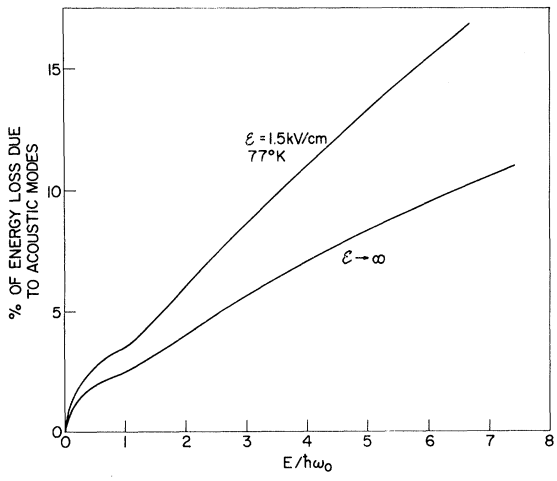

FIG. 7. Percent of the total energy loss due to the acoustic modes for $\mathcal{E} \to \infty$.

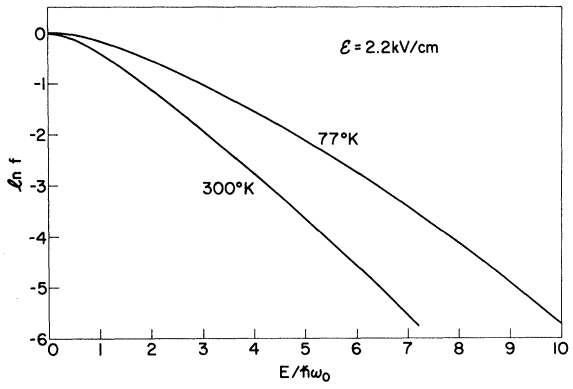

FIG. 8. Calculated electron distribution functions at 77 and 300 °K showing accelerated attenuation at higher energies due to nonparabolicity and acoustic-mode energy loss.

this transfer involves the majority of electrons as in GaAs, but at the higher field the drift velocity is no doubt affected by both the scattering between the ⟨111⟩ and ⟨100⟩ valleys and the partial population of the ⟨100⟩ valleys.

(iii) On either the intravalley or the electron transfer models of the negative resistance the vanishing of the negative resistance must be due to substantial electron transfer, since in our calculations there is no mechanism which causes the resistance to change from negative to positive at higher fields. The intravalley model presented here, however, would be consistent with the increase of the oscillation threshold with pressure observed by Melz and McGroddy.

Recently, Fawcett and Paige[21] have made Monte Carlo calculations of the drift velocity for n-type Ge. They have included the ⟨100⟩ valleys in their calculations but have not included those features of the ⟨111⟩ valleys which contribute to an intraband negative resistance. Any negative resistance they obtain is, of course, the result of electron transfer to the ⟨100⟩ valleys and depends upon the assumed properties of these valleys.

The parameters describing the ⟨100⟩ valleys in Ge are obtained from the information available about Si, and there is also some check from low-field hydrostatic pressure experiments,[22] which brings the ⟨100⟩ valleys below the ⟨111⟩ valleys in Ge. The major difficulties in such an approach are the following: (i) Our knowledge is still imperfect concerning the scattering mechanisms in Si; (ii) there is almost certainly a significant difference in the detailed description of the scattering and band structure of the ⟨100⟩ extrema in Si and Ge, e.g., the frequencies of the lattice vibrations spectrum of Si are approximately 70% greater than

in Ge; (iii) the observed negative resistance is not obtained in the calculations if a high probability for nonequivalent intervalley scattering is taken into account.

A dip in the low-field conductivity of Ge at hydrostatic pressures which cause the ⟨111⟩ and ⟨100⟩ acts of valleys to cross in energy indicates that the scattering probability between these sets of valleys in Ge is rather high. It is a curious result of theories involving electron transfer that the more easily carriers can scatter between nonequivalent valleys, the more remain behind in the lower valley (s) at a given field. Fawcett and Paige have noted that with a strong intervalley coupling constant it is difficult to obtain a negative conductivity at 77 °K because of the small amount of transfer.

A complete theory of the conductivity of electrons in Ge would need to consider the contributions to the conductivity of the both ⟨111⟩ electrons and the transferred electrons. In this paper we have considered the contribution of the ⟨111⟩ electrons and have shown that if the relevant details of the band structure and scattering mechanisms are taken into account, a negative resistance in good agreement with the observed I-V characteristics results. Although we have not included any effects due to electron transfer, we would conclude that a theory based primarily on electron transfer is perhaps more incomplete in its consideration of important mechanisms contributing to a negative resistance in Ge.

---

[1]J. C. McGroddy and M. I Nathan, IBM J. Res. Develop. 11, 337 (1967).
[2]B. J. Elliot, J. B. Gunn, and J. C. McGroddy, Appl. Phys. Letters 11, 253 (1967).
[3]D. M. Chang and J. G. Ruch, Appl. Phys. Letters 12, 111 (1968).
[4]See, for example, E. G. S. Paige, in *Progress in Semiconductors*, edited by A. F. Gibson and R. E. Burgess (Wiley, New York, 1964), Vol. 8, p. 191.
[5]P. J. Melz and J. C. McGroddy, Appl. Phys. Letters 12, 321 (1968).
[6]D. Brust, J. C. Phillips, and F. Bassani, Phys. Rev. Letters 9, 94 (1962).
[7]R. L. Aggarwal, M. D. Zuteck, and B. Lax, Phys. Rev. Letters 19, 236 (1967).
[8]G. Dresselhaus, A. F. Kip, and C. Kittel, Phys. Rev. 98, 368 (1955).
[9]G. F. Dresselhaus, Ph. D. thesis, University of California, 1955 (unpublished).
[10]E. O. Kane, J. Phys. Chem. Solids 1, 249 (1957).
[11]W. P. Dumke, Phys. Rev. 101, 531 (1956).
[12]D. Matz, Phys. Rev. 168, 843 (1968).
[13]F. J. Morin, Phys. Rev. 93, 62 (1954).
[14]H. B. Levinson, Fiz. Tverd. Tela 6, 2113 (1964) [Soviet Phys. Solid State 6, 1665 (1965)].
[15]W. P. Dumke, Phys. Rev. 167, (1968).
[16]J. B. Gunn, J. Electron. 2, 87 (1956).
[17]J. E. Smith, Phys. Rev. 178, 1364 (1969).
[18]W. Paul, J. Phys. Chem. Solids 8, 196 (1959).
[19]P. J. Price (unpublished).
[20]P. J. Price, in *Proceedings of the Ninth International Conference on Physics of Semiconductors*, edited by S. M. Ryvkin (Nauka Publishing House, Leningrad, 1968), Vol. 2, p. 753.
[21]W. Fawcett and E. G. S. Paige, Electron. Letters 3, 505 (1967).
[22]A. Jayaraman and B. B. Kosicki, in Ref. 20, Vol. 1, p. 53.